Developmental Biology 354 (2011) 67–76

Contents lists available at ScienceDirect

Developmental Biology

journal homepage: www.elsevier.com/developmentalbiology

Recapitulation of developmental cardiogenesis governs the morphological and functional regeneration of adult newt hearts following injury

Nevin Witman [a], Bari Murtuza [b], Ben Davis [c], Anders Arner [c], Jamie Ian Morrison [a,*]

[a] Molecular Biology and Functional Genomics, Stockholm University, 10691 Stockholm, Sweden
[b] Department of Paediatric Cardiac Surgery, Great Ormond Street Hospital for Children, London WC1N 3JH, UK
[c] Department of Physiology and Pharmacology, Karolinska Institutet, Stockholm SE-171 77, Sweden

ARTICLE INFO

Article history:
Received for publication 14 December 2010
Revised 18 March 2011
Accepted 22 March 2011
Available online 30 March 2011

Keywords:
Bromodeoxyuridine
Echocardiogram
Islet1
Resection
Reverse remodeling

ABSTRACT

Urodele amphibians, like the newt, are the "champions of regeneration" as they are able to regenerate many body parts and tissues. Previous experiments, however, have suggested that the newt heart has only a limited regeneration capacity, similar to the human heart. Using a novel, reproducible ventricular resection model, we show for the first time that adult newt hearts can fully regenerate without any evidence of scarring. This process is governed by increased proliferation and the up-regulation of cardiac transcription factors normally expressed during developmental cardiogenesis. Furthermore, we are able to identify cells within the newly regenerated regions of the myocardium that express the LIM-homeodomain protein Islet1 and GATA4, transcription factors found in cardiac progenitors. Information acquired from using the newt as a model organism may help to shed light on the regeneration deficits demonstrated in damaged human hearts.

Introduction

Adult human hearts have a very limited ability to generate new cardiac myocytes. Although this mechanism might be important for turnover or homeostasis of the cardiac cells, it has insufficient capacity for regenerating significant regions of the myocardium following injury (Bergmann et al., 2009; Torella et al., 2007). Instead of functional replacement of cardiomyocytes with electro-mechanical stabilization (reverse remodeling), the damaged myocardium is infiltrated by fibrotic tissue (Chachques, 2009). This type of wound healing response where the functional myocardium is replaced by the scar tissue may lead to progressive heart failure. Experimental and clinical trials involving the use of cell-based therapies, delivery of growth factors and cardiac tissue engineering are producing promising but conflicting results (Bartunek et al., 2009; Genovese et al., 2007; Reffelmann et al., 2009). Along with identifying the optimal cell type to transplant, with respect to stage of commitment or diversification within a myocardial sub-lineage, there still remain the issues of cell delivery, homing of the cells to the damaged areas of the heart and electrical coupling into the host myocardium that have to be addressed before cell-based therapies can be considered as a suitable substitute to established heart intervention therapies (Mummery et al., 2010).

In order to address these problems it is necessary to obtain information from organisms that can regenerate the myocardium following damage. Some elegant work has recently shown that the two-chambered heart of the zebrafish can undergo extensive regeneration following injury (Poss et al., 2002). Another species that has comprehensive regeneration abilities is the red-spotted newt or *Notophthalmus viridescens* (Brockes and Kumar, 2002). This urodele amphibian has the remarkable ability to regenerate multiple organs and tissues, with the most impressive example being the regeneration of a fully functioning limb following amputation (Brockes, 1997). However, earlier studies concluded there was a regeneration deficit when it came to cardiac repair in these animals (Becker et al., 1974; Neff et al., 1996; Oberpriller and Oberpriller, 1974).

There have been some intriguing results indicating that the newt heart does have an ability to repair. For example, if minced newt cardiac tissue is transplanted to the site of a resected ventricle, not only is there increased proliferative events at the transplantation site but there is also functional integration and restoration of the resected newt ventricle (Bader and Oberpriller, 1978). Furthermore, it has been shown that following crush injury to the newt ventricle there is a severe reduction in sarcomeric proteins, with levels of these proteins restored several weeks following the initial injury (Laube et al., 2006). However, many of the heart regeneration models in the newt remain poorly characterized in terms of cellular contribution and length of time necessary to restore a fully functioning myocardium following injury.

To address the extent of regeneration in the newt heart, we have developed a standardized ventricular resection model in the red-spotted newt (*N. viridescens*) where we can follow functional and structural restoration for extended periods of time after the initial injury. We show via histological and functional echocardiogram

* Corresponding author at: Molecular Biology and Functional Genomics, Stockholm University, Svante Arrheniusväg 20C, 10691 Stockholm, Sweden. Fax: +46 8 166488
E-mail address: jamie.morrison@molbio.su.se (J.I. Morrison).

0012-1606/$ – see front matter © 2011 Elsevier Inc. All rights reserved.
doi:10.1016/j.ydbio.2011.03.021

analysis that the newt heart morphologically and functionally regenerates, without the presence of scarring. We further show the identification of separate populations of proliferating Islet1 and GATA4 positive cells within the regenerating regions of the heart, implying that cardiac progenitors could be present and participate in the regeneration of newt myocardium.

Materials and methods

Antibodies

The following primary antibodies were used: mouse monoclonal anti-myosin heavy chain IgG (MF20; Developmental Studies Hybridoma Bank), mouse monoclonal anti-Islet1 IgG (40.2D6; Developmental Studies Hybridoma Bank), goat polyclonal anti-cardiac troponin T (Abcam plc, UK), rat monoclonal anti-BrdU IgG (Trichem ApS), rabbit polyclonal anti-GATA4 (H-112), mouse monoclonal anti-GATA4 (G4), rabbit polyclonal anti-NKX2.5 (H-114) and rabbit polyclonal anti-p-Histone H3 (Ser 10) (GATA4, NKX2.5 and Histone H3 antibodies are from Santa Cruz Biotechnology). For immunofluorescence studies, primary antibodies were detected with appropriate species-specific Alexa Fluor-conjugated secondary antibodies (Invitrogen).

Animals and procedures

All experiments were performed according to European Community and local ethics committee guidelines. Adult red-spotted newts, *N. viridescens*, were supplied by Charles D. Sullivan Co., Inc. and maintained in a humidified room at 15–20 °C. Newts were anesthetized by placing them in an aqueous solution of 0.1% ethyl 3-aminobenzoate methanesulfonate salt (Sigma-Aldrich) for 15 min. Newts were positioned supine and an incision was made into the ventral body wall exposing the pericardium. The thoracic cavity was exposed fully with a single anchoring stitch, using a reverse cutting (3/8 circle 8 mm) needle with monofilament 8.0 non-absorbable suture, placed into both sides of the incised pericardium. Blunted 5.0 forceps were placed under the exposed aorta, and lifted, in order to expose the heart exteriorly. Starting just below where the atria enter the ventricle, a 27 G needle (0.41 mm) was then used to make a diagonal left to right puncture of the ventricle wall. Using iridectomy scissors, the portion of the tissue pierced by the needle was removed from the ventricle. Hemorrhaging was stemmed via rapid clot formation, brought about by the application of local pressure with cotton swabs. The damaged hearts were maneuvred back into the thoracic cavity and the pericardium and body wall were closed with interrupted stitches using sutures previously mentioned. Newts were left to recover for 24 h in an aqueous solution of 0.5% sulfamerazine (Sigma-Aldrich) on ice, before being placed back into a 15–20 °C water environment. Heart masses were measured using a Sartorius electron microscope (BP210D), which has a readability of 10 μg. For BrdU labeling experiments animals were injected intraperitoneally with 25 μl of 2 mg/ml BrdU 1 day, 3 days, 7 days, 10 days, 14 days and then weekly up until indicated time-points.

Echocardiogram analysis

The ultrasonic imaging was performed on anesthetized newts using a Philips HDI 5000 system with a CL 15–7 probe. Each recording was performed within 15 min after onset of anesthesia. The diastolic and systolic diameters were measured blindly, with at least three recordings made on each animal at each session. The average value was used as a representative recording for the animal at each specified time-point. Fractional shortening measurements were made using the following equation:

$$((\text{Diastole}-\text{Systole})/\text{Diastole})\times 100 = \text{Fractional shortening}(\%).$$

To compare mean fractional shortening percentages between uninjured and resected hearts, a Mann–Whitney *U* test was performed. Statistical significance was accepted at $P<0.05$.

RNA extraction and cDNA synthesis

RNA was extracted from newt A1 myoblasts and ventricular myocardium using the RNAqueous®-4PCR kit (Ambion) according to the instructions of the manufacturer. Ventricular myocardium was obtained by dissecting newt hearts free from the thoracic cavity and removing the connecting aorta and atria with micro-surgical scissors. One microgram of total RNA was used for cDNA synthesis, performed in a 25 μl reaction using 0.8 mM dNTPs, 2 μg 3′RACE Adaptor (Ambion), 1× first strand buffer, 10 U RNase Inhibitor (Invitrogen) and 50 U M-MuLV reverse transcriptase (Fermentas). RNA, primers and dNTPs were first incubated at 37 °C for 90 min followed by 70 °C for 10 min cycle to heat-inactivate the transcriptase. The reaction mixture was diluted with 25 μl of 1× first strand buffer. For every RNA sample, a negative control, lacking reverse transcriptase, was also performed.

PCR protocols

Partial cDNAs for cardiac transcription factors from *N. viridescens* were cloned using degenerate PCR (Table 1). All PCRs were carried out using High Fidelity PCR Enzyme Mix (Fermentas) according to manufacturer's instructions. Primers against the partial cDNA sequences for NKX2.5 (HM367109), GATA4 (HM367110), GATA5 (HM367111), HAND2 (HM367112) and Islet1 (HM367113) were designed using Primer-BLAST (NIH) and Oligo Property Scan (Eurofins MWG Operon—Table 2). For the semi-quantitative PCR, 1 μl of cDNA was mixed with 0.2 μM of each primer, 0.4 mM of each dNTP, 1.5 mM $MgCl_2$, 1× PCR buffer with $(NH_4)_2SO_4$ and 1 U Taq DNA Polymerase (recombinant—Fermentas) in a 25 μl reaction. After an initial denaturation step at 94 °C for 2 min, the samples were put through 10 cycles of 94 °C for 15 s, 60 °C for 30 s and 72 °C for 10 s, followed by 19–25 cycles of 94 °C for 15 s, 55 °C for 30 s and 72 °C for 10 s, followed by a final elongation step at 72 °C for 10 min. Comparative samples were run on 2% agarose gels containing ethidium bromide and visualized on a UV table. Real-time PCR was carried out using Fast qPCR 2× buffer (KAPA Biosystems, USA) on a Qiagen Rotor-Gene Q real-time PCR machine, according to manufacturer's instructions. Real-time PCR expression analysis of each gene was normalized to GAPDH, a ubiquitously expressed gene used previously as a normalization factor (Vascotto et al., 2005). Eurofins MWG Operon supplied all primers used. To compare mean relative gene expression between uninjured and resected hearts, a two-tailed Student's *t*-test was performed. Statistical significance was accepted at $P<0.05$.

Histology

Tissue samples were mounted as previously described (Morrison et al., 2006). Six micrometer frozen serial sections were cut through the entire ventricle using a Leica Jung CM1800 cryostat. A hematoxylin and eosin (H&E) staining was performed to observe overall cardiomyocyte and nuclei structure. Acid fuchsin-orange G staining (AFOG), which

Table 1
Degenerate primers used to identify cardiac transcription factors.

Gene	Forward	Reverse
Islet1	5′-TCNCCGGAYYTGGARTGGCA-3′	5′-CANCKCTTGTTYTGAAACCA-3′
NKX2.5	5′-CAGGTNAARATHTGGTT-3′	5′-ACCADGCYCKDATBCCATG-3′
GATA4	5′-GGMYTNTAYCAYAAGATGAA-3′	5′-GCYARGACCAGGYTGTTCCA-3′
GATA5	5′-CAAAGCTTTAYCAYAARATGAA-3′	5′-TCGAATTCCCRTGNARCTTCAT-3′
HAND2	5′-GAGTGCATCCCCAAYGTKCC-3′	5′-CCAKACYTGCTGVGGCCA-3′

Table 2
PCR primers for cardiac transcription factors.

Gene	Forward	Reverse	Size
Islet1	5′-TGCACTGCGGGAAGACGGAC-3′	5′-GTCGGAGAGCGGGCTGCCTA-3′	155 bp
NKX2.5	5′-GACAGCGGCAGGACCAGACC-3′	5′- GGCATTGCATGCAGGGCTTGTG-3′	188 bp
GATA4	5′-GGGTGCCAAGGCCACTAGCAATG-3′	5′-GGGCGCAGGTCTTCTGTGGTGAC-3′	172 bp
GATA5	5′-AACGGCATCAACCGGCCCCT-3′	5′-CAAGCCGCAAGCGTTGCACA-3′	150 bp
HAND2	5′-TTGCGCTTGTCCTCCTTGCCG-3′	5′-CCGACACCAAGCTCTCCAAGATCA-3′	151 bp
GAPDH	5′-TGTGGCGTGACGGCAGAGGTG-3′	5′-TCCAAGCGGCAGGTCAGGTCAAC-3′	166 bp

stains fibrin red and collagen bright blue, was performed as described previously (Poss et al., 2002).

Immunofluorescence

Immunofluorescence of cryosections was performed as previously described (Morrison et al., 2010). For stainings involving the use of secondary donkey anti-goat fluorescent antibodies, 10% swine serum replaced 10% goat serum as the block buffer. For confocal images the mounting media contained 1 μM TO-PRO3 iodide (Invitrogen). BrdU and phosphorylated histone 3 counts were performed on at least 3 sections per animal spanning an approximate distance of 150 μm through the regenerating ventricular myocardial area.

Microscopy and image processing

An LSM 510 Meta laser microscope with LSM 5 Image Browser software (both Carl Zeiss MicroImaging, Inc.) was used for confocal analyses. A microscope (Axioplan 2; Carl Zeiss MicroImaging, Inc.) with Axiovision 4 software (Carl Zeiss MicroImaging, Inc.) was used for epifluorescence microscopy analyses. A Leica DC 300 F camera mounted to a Reichert–Jung Polyvar microscope with LEICA IM 500 software was used for brightfield microscopy analyses. A NIKON Coolpix 4500 digital camera mounted to a Zeiss stemi 2000-c dissecting microscope was used for gross morphology image analyses. Images were taken at room temperature and were further processed using Photoshop (Adobe) by linear adjustments.

Results

Morphological repair of resected newt hearts

In order to address the regenerative capacity of the newt heart following ventricular resection, we developed a new surgical method aimed at removing a segment of the heart in a more standardized and reproducible manner. We resected a lateral portion of the ventricle, located near the boundary of where the atria enter the ventricle, using a 27 G needle as a template to precisely control the area to be resected (Supplementary Fig. 1). By resecting a more lateral region of the ventricle, as opposed to the apex, we minimized the possibility of breaching the ventricular cavity. Furthermore, the 27 G needle provided a controlled method of isolating a piece of ventricle to remove more precisely, without having to rely on timing the resection based on the contractions of the heart. This resulted in the consistent removal of ventricular myocardium (145 ± 53 μg) with carefully defined dimensions (equivalent to removing between 5%–10% total ventricular myocardium based on an average ventricle mass of 2.0 ± 0.3 mg). This method proves very successful, with only a 4% mortality rate (from a total of 94 resections).

Gross morphology of the newt heart following resection consistently shows a large area of damage 7 days post-injury, with a gradual restoration of the myocardial tissue over time (Fig. 1A). It is difficult to see the original area of damage at the latter time-points of 60 days post-resection. Hematoxylin and eosin (H&E) and acid fuschin-orange G (AFOG) staining of sections reveal large deposits of fibrin (red staining) and collagen (blue staining) at 7 days post-resection, with the fibrin clot receding over the next 14 days (Fig. 1B–D). Three to four weeks post resection the epicardium is restored and over the course of the next 40–50 days the mononuclear infiltrated damaged area and matrix deposition is gradually replaced with cardiomyocytes, reminiscent of the infiltrating pink cardiomyocyte tissue seen in Fig. 1A. At 60 days, the majority of the resected myocardium has been replaced with cardiomyocytes, with minimal signs of reverse remodeling and no visible signs of scarring. These results demonstrate that newt myocardium is restored, without scarring, following resection injury.

Functional restoration of newt myocardium

To be able to claim that the newt heart can fully regenerate following resection injury, cardiac functional tests were performed in order to demonstrate that the new myocardium had functionally integrated at the site of the initial damage and could contribute to the contractility of the ventricle. In order to assess functional output during the regeneration of the newt heart, we employed echocardiographic analysis to measure ventricular performance by comparing fractional shortening values from uninjured controls with animals at various time-points following resection (Fig. 2). The probe was advanced from the abdominal side in the cranial direction and when cardiac movements were observed the probe was positioned so that the diastolic diameter was maximal. Fig. 2A shows M-mode ultrasonic recordings of the ventricle in an uninjured newt. To confirm that the dimensions recorded were in the correct range, digital photographs were taken of the exposed heart during diastolic and systolic contractions (Fig. 2B). The outer diameters were approximately 0.26 and 0.20 cm in diastole and systole, respectively. These diameters are slightly larger than those of the echocardiographic recording, which suggest that the latter method monitors motions of the inner cardiac wall.

Ten newts were used for diastolic and systolic measurements of the inner cardiac wall (Fig. 2C and Supplementary Table 1) and fractional shortenings were calculated (Fig. 2D). Uninjured newts had an average fractional shortening of approximately 37.5%, which is in accordance with optical coherence tomography measurements of fractional shortening taken from *Xenopus laevis* (Boppart et al., 1997). There was a significant 10% reduction in fractional shortening 7 days following injury, indicating a decrease in cardiac function. The fractional shortening at 23 and 60 days post-resection resembled that of an uninjured, with the 60-day time-point showing a significant increase when compared to the 7-day time-point. The variable increase in cardiac function observed at 23 days post-resection coincides with newly regenerated epicardium (Fig. 1B and C). The epicardium provides a mechanical integrity to the myocardium, facilitating the contraction and relaxation of the heart (Jobsis et al., 2007). Therefore, it could be possible that the restoration of the epicardium imparts a structural stability resulting in an improvement in heart movement and function. However, as can be seen with the lack of significance at 23 days post-resection, restoration of this epithelial connective tissue layer alone is insufficient for significant functional recovery.

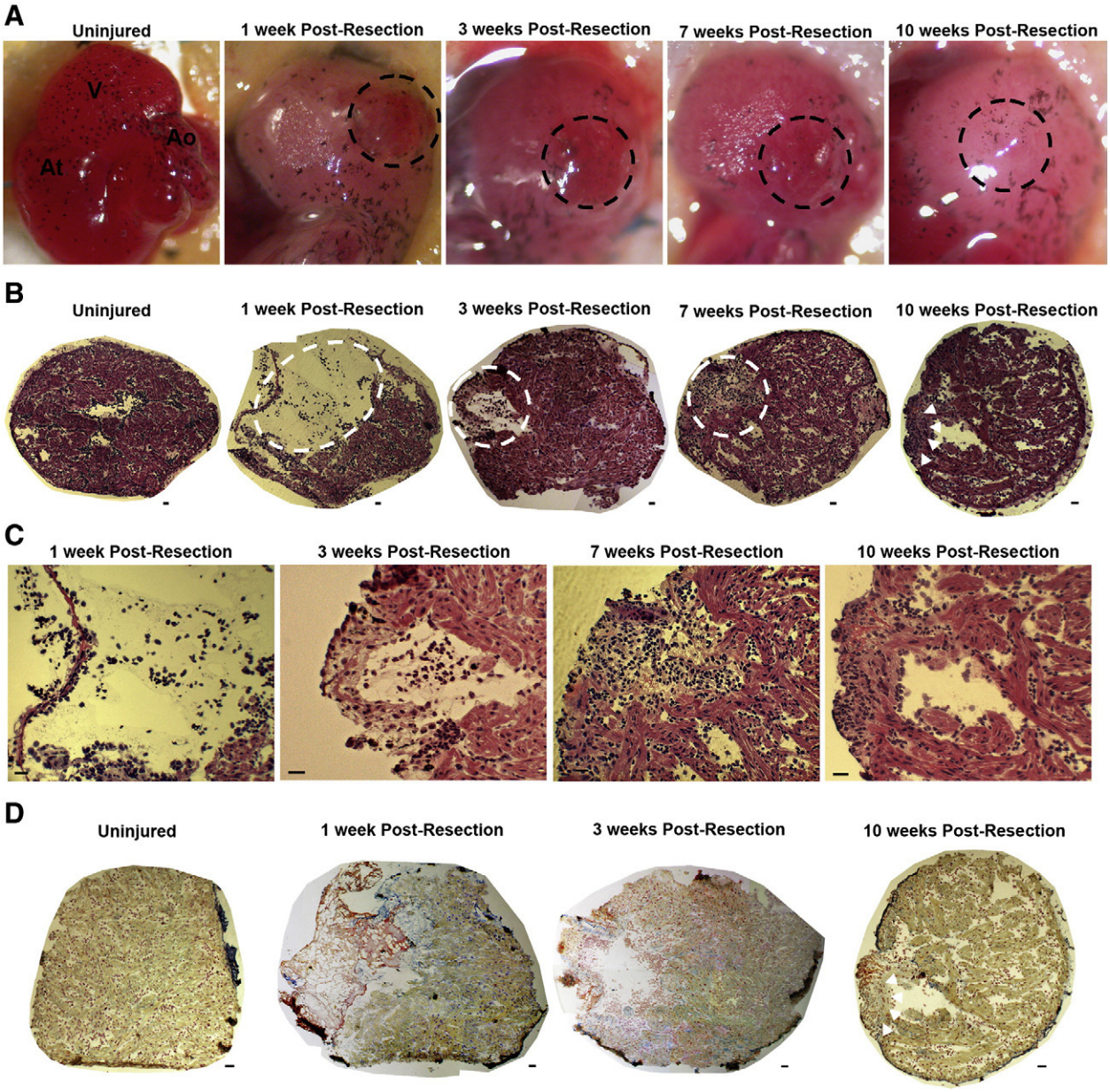

Fig. 1. Morphological regeneration of the newt ventricular myocardium following resection. (A) Representative digital photographs of exposed uninjured and resected newt hearts at indicated time-points. The broken outline black circular boundaries indicate the position of the injury. V—ventricle; Ao—aorta; At—atrium. (B–D) Representative composite photomicrographs of complete transverse cryosections taken through the ventricular myocardium at indicated time-points, stained with hematoxylin and eosin (B–C) and acid-fuschin orange G (D). Broken outline white circular boundaries in (B) indicate the progression of reverse remodeling following resection (regeneration zone). The white arrows in (B) and (D) indicate minor reverse remodeling is still occurring. (C) Higher resolution photomicrographs of the reverse remodeling demarcated in (B). Scale bars are 50 μm.

Echocardiographic analysis also revealed a consistent heart rate for all non-injured and injured time-points analyzed, (ranging from 58–62 beats per minute), suggesting that the cardiac pacemaker regions are not impaired and that the altered cardiac shortening fraction is not compensated by increased heart rate in the injured newt heart. These results indicate that the newt myocardium restores its functional ability within 60 days, following resection injury.

New myocardium contains proliferating cells

To ascertain whether the newly formed myocardium was the result of a hypertrophic regenerative response or the activation of cells to re-enter the cell cycle, we performed BrdU pulse chase experiments with newts that had undergone ventricular resection (Fig. 3A and B). We conducted an elongated BrdU pulse chase experiment in order to catch cells at earlier and later time-points that could be responsible for the regeneration we were observing. Using antibodies directed against myosin heavy chain, which detects mature cardiomyocytes, and BrdU, we observed a gradual increase of both BrdU positive cardiomyocytes and non-cardiomyocytes populations (Fig. 3C). BrdU positive non-MHC-expressing cells were present throughout the heart section, with an increased presence around the injury site. We saw a peak of cellular proliferation between 30–45 days post-resection, with BrdU positive non-cardiomyocyte numbers gradually returning to levels found in the uninjured heart at later time-points. The majority of BrdU positive cardiomyocytes were located at the boundary of the injury, which becomes more apparent at 45 days post-resection and at later points.

Using an antibody directed against phosphorylated histone 3 (H3P) we could also detect cardiomyocytes undergoing mitosis (Fig. 3D). In accordance with the BrdU labeling pattern, albeit with expectedly fewer observed numbers, we show a peak of H3P positive

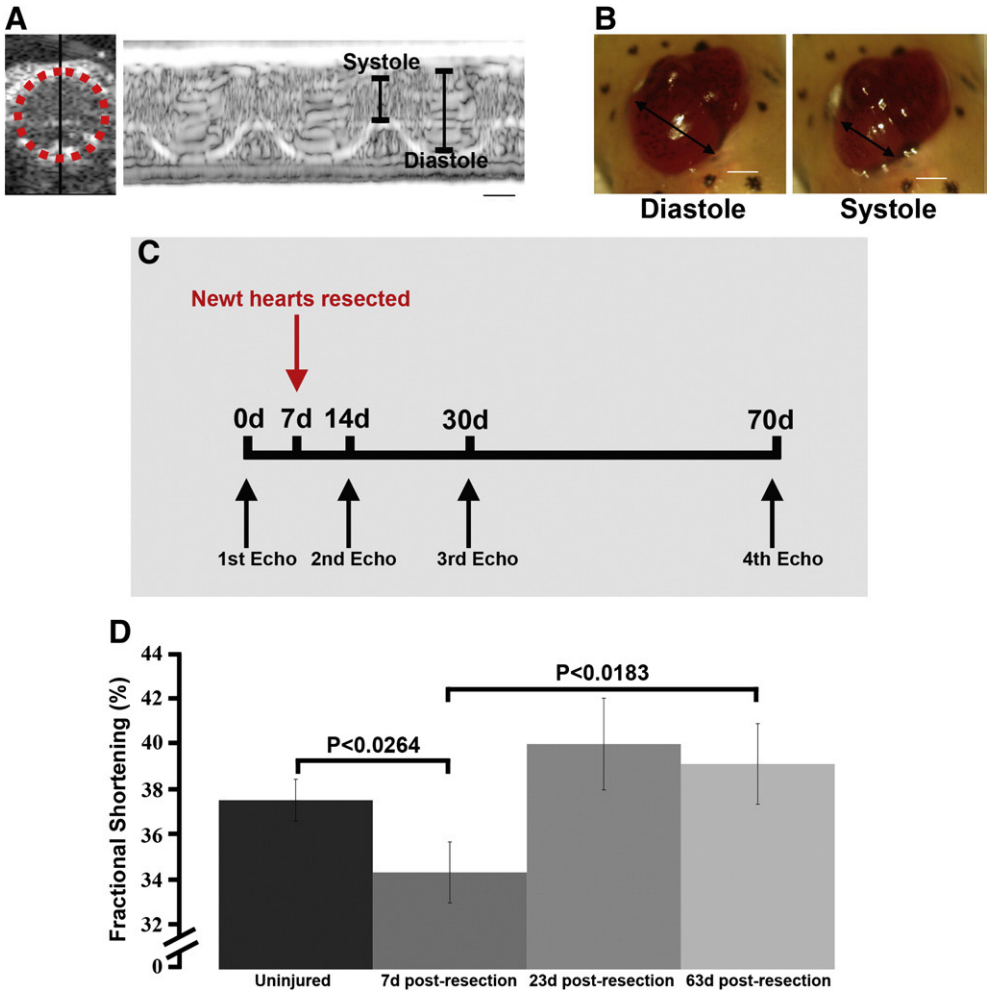

Fig. 2. Echocardiographic analysis of functional regeneration in the newt heart following resection. (A) Original M-mode traces from a non-operated newt and the resulting trace leading to end-diastolic and end-systolic diameters. The dashed red circle and the solid black line indicate the boundaries of the ventricle and the orientation of the probe, respectively. (B) Digital photographs of an exposed newt ventricle in diastolic and systolic positions. The double-ended arrows represent the axis at which the probe was positioned. (C) Schematic diagram detailing the echocardiogram time-points. (D) Fractional shortening measurements of the uninjured and resected newt hearts at indicated time-points. Error bars are s.e.m. *P* value is from a Mann–Whitney test. Scale bars are 0.5 mm.

cardiomyocytes and non-cardiomyocytes between 10–21 days post-resection, with this number decreasing to levels seen in uninjured newt hearts at later time-points (Fig. 3E). The increased presence of cell proliferation, as indicated by the BrdU and H3P stainings, indicates that the cells contributing to the repopulation of the resected area of myocardial tissue is due to both cardiomyocyte and non-cardiomyocyte derived cells. Furthermore, the persistent expression of BrdU at later time-points compared to H3P implies that the cells dividing at the earlier time-points are the major contributors to the newly regenerated myocardial tissue.

Molecular signature of heart regeneration

Cardiogenesis requires the coordinated expression of specialized transcription factors to drive cardiac specification in the cells responsible for forming the structures of the heart (Harvey, 2002). In order to see if the transcriptional regulation of newt heart regeneration follows a similar expression profile as cardiogenesis, we used degenerate PCR to clone out the cardiac transcription factors *NKX2.5*, *GATA4*, *GATA5*, *Islet 1* and *HAND2* (Brade et al., 2007; Brand, 2003; Srivastava et al., 1995). Real-time RT-PCR was performed in order to obtain comparative expression levels at time-points during regeneration (Fig. 4). RNA from the ventricular myocardium was used for RT-PCR and semi-quantitative PCR was performed to confirm that the primers used for the real-time PCR produced single band products at the expected size (Supplementary Fig. 2).

Overall, we saw a similar expression pattern for all cardiac transcription factors, with a decrease in expression at 7 days post-resection followed by an increase at 23 days post-resection. HAND2, GATA4 and GATA5 demonstrated the most dramatic increases, especially for GATA4, with expression levels significantly higher than that seen in control uninjured hearts. Interestingly, this is a time-point when proliferation events are at their peak, indicating that there could be a correlation between the activation of the cell cycle and expression of cardiac transcription factors. At 45 days post-resection there was a consistent significant drop in expression compared to control uninjured hearts, again indicating that the cells responsible for the replacement of functional cardiomyocytes are determined and no longer need the over-expression of these transcription factors.

GATA4 and Islet1 non-cardiomyocytes identified within the regenerating newt myocardium

The increase in cardiogenic transcription factor mRNA expression during the proliferative phase of regeneration is interesting, as this could be an indicator for the presence of specialized cells within the newt heart that are responsible for the newly regenerated myocardium. In order to verify the mRNA expression data with protein

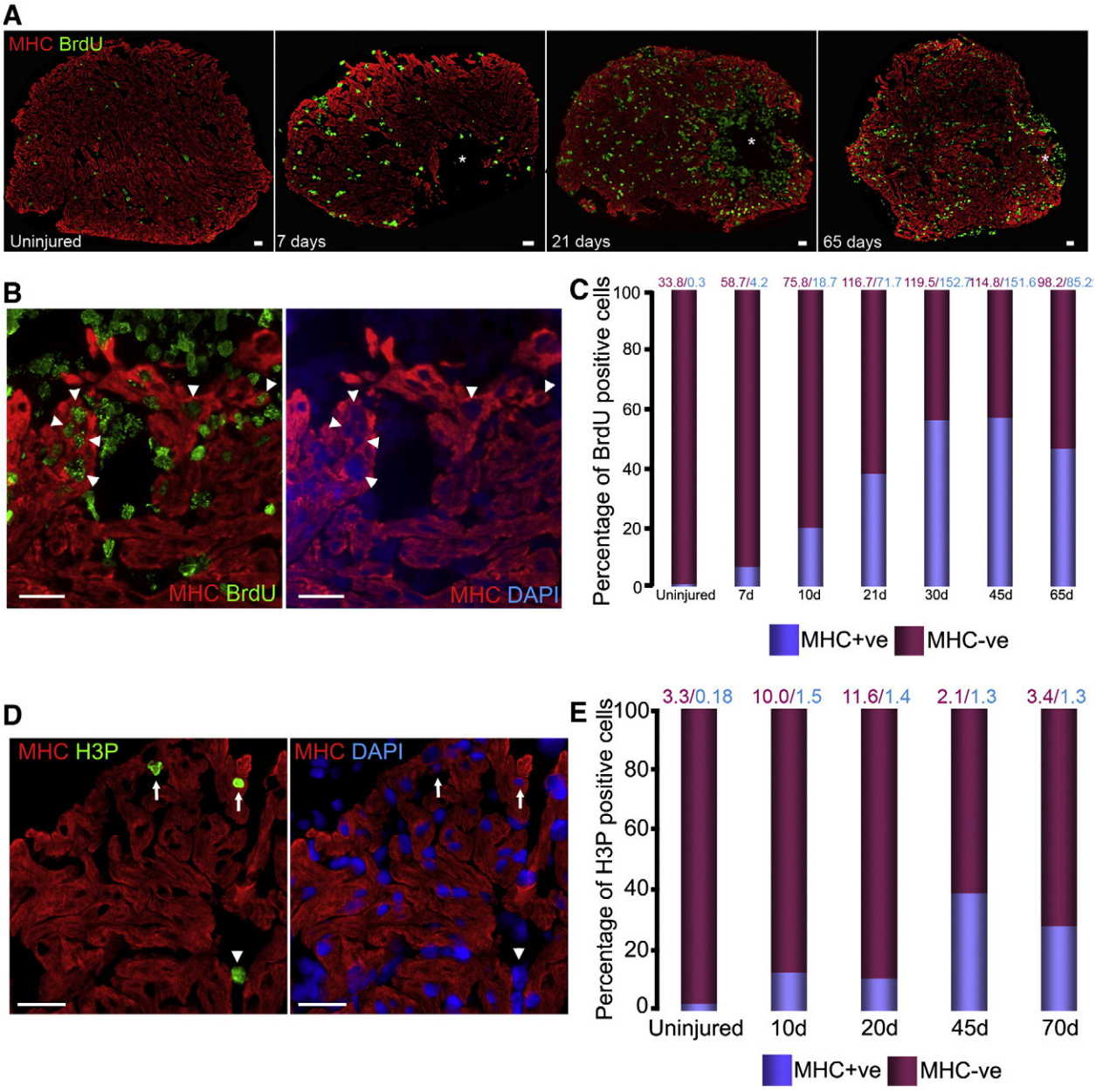

Fig. 3. Resection of the newt heart results in increased proliferative events. (A and B) Representative photomicrographs of newt ventricles immunolabeled with MHC and BrdU at indicated time-points. Asterisk indicates the area of damage following resection. (B) Higher magnification photomicrograph of a 65-day post-resected ventricle. The arrowheads show $MHC^{+}BrdU^{+}$ cells. (C). Graphical representation of the percentage of BrdU positive cells in uninjured and resected newt hearts. Three animals were used for each time-point, except 7, 10 and 30 days post-resection where 2 animals were used. (D) Representative photomicrographs of a 70 days post-resected ventricle immunolabeled with MHC and H3P. The arrows and arrowhead show $MHC^{+}H3P^{+}$ and $MHC^{-}H3P^{+}$ cells, respectively. (E) Graphical representation of the percentage of H3P positive cells in uninjured and resected newt hearts. Two animals were used for each time-point. The numbers above the bars in (C) and (E) represent the average number of cells counted per section. Scale bars are 50 μm.

expression, we immunolabeled ventricles from uninjured and injured hearts (7, 21, 45 and 60 days post-resected) to see if we could identify cellular expression of the transcription factors Islet1, GATA4 and NKX2.5. Ventricular cardiomyocytes from all time-points studied, labeled with antibodies directed against cardiac troponin T and myosin heavy chain, co-expressed GATA4, NKX2.5 and Islet1 (Fig. 5 and Supplementary Fig. 3). The expression of all transcription factors remained localized to the nuclei of cardiomyocytes and was present throughout the ventricular myocardium. The Islet1 expression was verified by immunolabeling without primary antibodies, as well as analyzing wavelength emission spectra to distinguish Alexa 488 fluorescence from non-specific autofluorescence (Supplementary Fig. 4) (van Laake et al., 2007).

Interestingly, GATA4 and Islet1 expression were not solely localized to cardiomyocytes. At 21 days post-resection GATA4 positive non-cardiomyocytes were identified, concentrating adjacent to the newly regenerated cardiomyocytes in the regeneration zone (Fig. 5C–E and Supplementary Fig. 3G–I). Approximately 20% of the non-cardiomyocytes in the regeneration zone expressed GATA4. In addition, a separate population of Islet1 positive non-cardiomyocytes was identified, concentrating around the epicardial region of the regenerating zone (Fig. 5F–K). Approximately 30% and 10% of the non-cardiomyocytes in the regeneration zone expressed Islet1 at 21 and 45 days post-resection, respectively. GATA4 and Islet1 non-cardiomyocytes were never observed in uninjured or resected newt hearts at all other time-points studied. NKX2.5 expression was localized exclusively to the

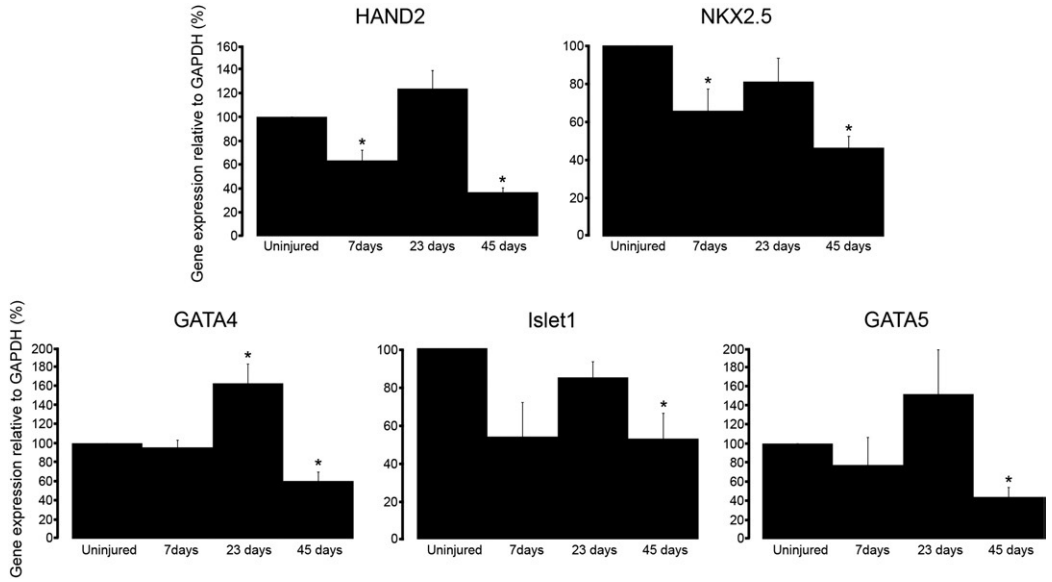

Fig. 4. Increased mRNA expression of cardiac transcription factors coincides with elevated proliferation. qRT-PCR Analysis of cardiac transcription factor mRNAs relative to GAPDH in uninjured and resected newt hearts at indicated time-points. Error bars are s.e.m. * Indicates significance against relative gene expression values in uninjured hearts. Relative expression levels were obtained from averaging five separate qPCR runs for every gene analyzed, except GATA5 and Islet1, where four and three runs were used, respectively.

ventricular cardiomyocytes at all time-points studied (Supplementary Fig. 3A–F). Co-localization of BrdU expression within the GATA4 and Islet1 non-cardiomyocyte populations shows that these cells are actively proliferating during the regeneration of the myocardium (Fig. 5C–K). The presence of proliferating GATA4 and Islet1 non-cardiomyocytes in the regenerating zone of the ventricle indicates that the cells of newt heart could act as cardiac progenitors during proliferative phases of cardiac regeneration.

Discussion

The value of using the vertebrate adult newt as a comparable model system for mammalian regeneration is unquestionable. However, it was generally believed that the heart of the newt is one of the few organs that have a limited regeneration capacity. By using a novel surgical resection technique to precisely define the extent of resected tissue, and by looking at functional and morphological endpoints of the regenerative response, we have shown that following resection of the ventricular myocardium, the newt is capable of replacing cardiac tissue without permanent scarring. The fibrin and collagen deposited at early stages of the regeneration after cardiac resection in the newt resembles the unyielding scar formed following naturally- or artificially-induced myocardial infarction in mammals (Weber, 1989). In light of these similarities, albeit via two completely different injury methods, the newt heart resection model we have developed could be used to answer important questions such as why newts can replace dense extracellular matrix with functional myocardium following injury, whereas mammals cannot.

The scarless heart regeneration we report here initially seem at odds with earlier resection studies performed on newt hearts, which report the limited proliferation of cardiomyocytes infiltrating the scar tissue that replaces the damaged area of the heart (Becker et al., 1974; Neff et al., 1996; Oberpriller and Oberpriller, 1974). However, the majority of these studies terminated the experiments very early with 30 days post-resection being the latest time-point reported. This is a rather short time to take into account not only the functional regeneration of the heart but also the reverse remodeling that has to take place in order to regain morphological restoration comparable to that of an uninjured heart. This is further exemplified when considering that the regenerating newt limb takes approximately 25–30 days to gain full function following amputation, with a further several weeks needed to remodel back to a size comparable to an uninjured limb (Iten and Bryant, 1973). In addition, earlier studies remove the apex of the ventricle, whereas we chose another area to amputate. This might in turn reflect the presence of mature cardiac myocytes sub-populations responsible for the regenerative response being localized to discrete anatomical compartments within the heart (Beltrami et al., 2003; Kikuchi et al., 2010). Our method provides a stable platform to remove comparable amounts of tissue without relying on timing the resection based on cardiac rhythm. This again removes the variability of resection, which can influence greatly the extent of regeneration that can be performed. Furthermore, echocardiogram analysis allows us to non-invasively determine the progression of regeneration, which could be useful when assessing extrinsic up- or down-stream effectors of reverse remodeling in the newt.

In agreement with other cardiac regeneration models in the newt and zebrafish (Flink, 2002; Oberpriller et al., 1995; Poss et al., 2002), we do see a definite increase in cellular proliferation, with the peak occurring between 20 and 45 days post-resection. Even though the majority of these cells remain unidentified, we do see an increase in cardiomyocytes that are proliferating or have once undergone proliferation based on H3P and BrdU immunolabeling, respectively. However, these results contradict what happens with mammalian cardiomyocytes, which switch from hyperplastic to hypertrophic myocardial growth shortly after birth (Pasumarthi and Field, 2002). There has been some evidence of dividing cardiomyocytes following myocardial infarction in adult mammals, but the general consensus is that this low level of proliferation is temporally and spatially restricted and cannot contribute to a regenerative response (Beltrami et al., 2001; Yuasa et al., 2004). If comparisons between newts and mammals can be made, this could mean that newts have an ability to recreate a developmental cardiogenic milieu following injury, conducive to cardiomyocyte proliferation. Earlier work using different cardiac injury models in the newt postulated that cardiomyocytes are able to dedifferentiate and contribute to regenerating the damaged areas of the heart (Laube et al., 2006). Furthermore, work using cardiac regeneration models developed in neonatal mice and zebrafish has shown that specialized cardiomyocytes are able to proliferate and contribute to the regenerated cardiac tissue (Jopling et al., 2010; Kikuchi et al., 2010; Porrello et al., 2011). However, we

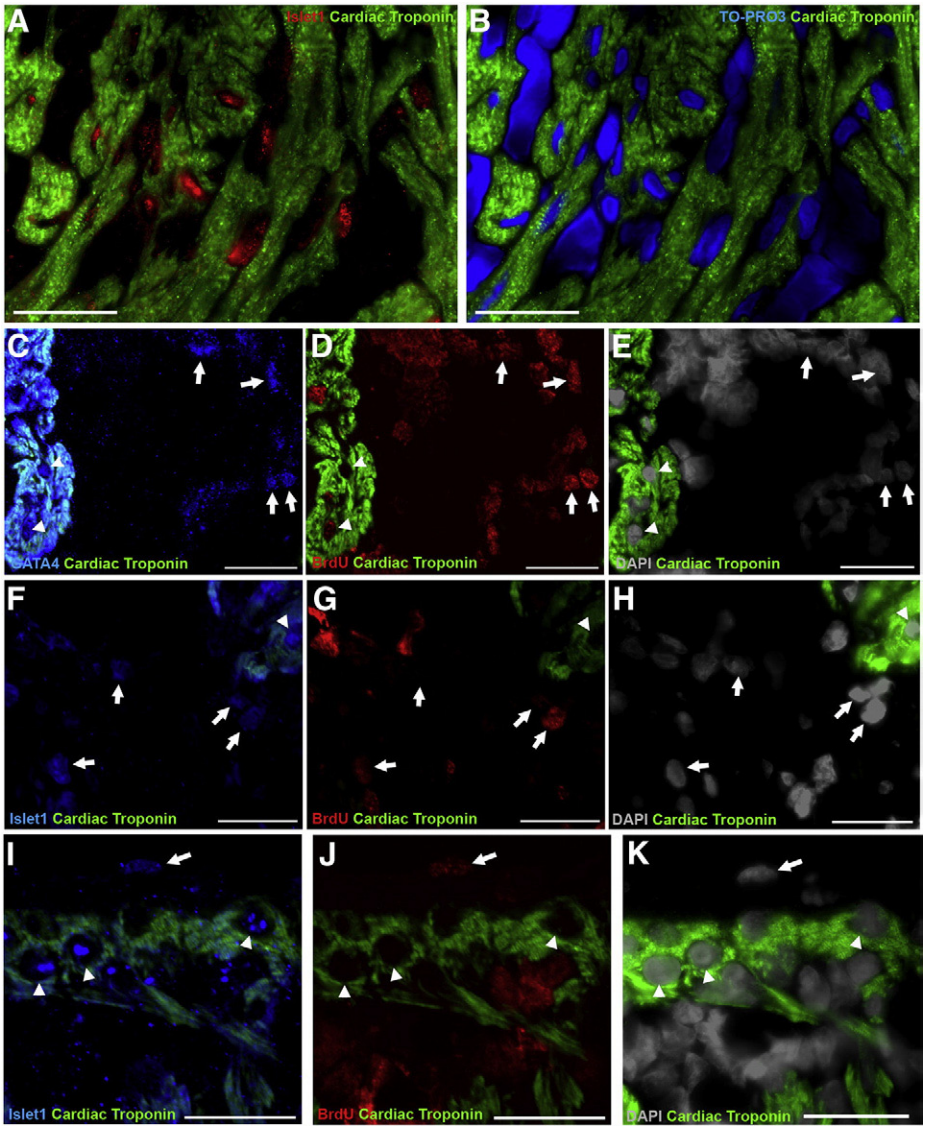

Fig. 5. Islet1 and GATA4 positive cells at the site of regeneration. (A–K) Representative photomicrographs of transverse cryosections of uninjured (A–B) 21-day (C–H) and 45-day (I–K) post-resection ventricles, immunolabeled with GATA4, Islet1, BrdU and cardiac troponin. (C and D), (F and G) and (I and J) are confocal images to the corresponding epifluorescent images shown in (E), (H) and (K), respectively. The arrows indicate cardiac troponin^{-} cells co-expressing either GATA4 (C–E) or Islet1 (F–K). The arrowheads indicate cardiac troponin^{+} cells co-expressing either GATA4 (C–E) or Islet1 (F–K). Scale bars are 50 μm.

cannot categorically claim that cardiomyocytes are the sole cellular component of the cardiac regeneration we have observed. Resident cardiac stem/progenitor cells have been identified in postnatal and adult mammals, suggesting a regenerative cell source that could be activated and home to areas of damage (Beltrami et al., 2003; Laugwitz et al., 2005; Martin et al., 2004; Oh et al., 2003). Using our model system, we are currently performing lineage-tracing experiments to identify whether cardiomyocytes dedifferentiate and contribute to the regenerated area or whether specialized cardiac progenitor cells influence the regeneration.

One aspect we can be certain of is the coordinated transcriptional up-regulation of cardiac transcription factors at a time when DNA synthesis and mitosis are at their peak. It is somewhat surprising that when proliferation begins to subside we see an overall down-regulation of cardiac transcription factors to expression levels lower than that seen in uninjured hearts. However, it has been shown previously that persistent over-expression of cardiac transcription factors like NKX2.5 and GATA4 in adult mice is linked to cardiac hypertrophy (Kasahara et al., 2003; Saadane et al., 1999). In addition, over-expression of NKX2.5 in xenopus and zebrafish embryos results in enlarged hearts (Chen and Fishman, 1996; Cleaver et al., 1996). So the sudden down-regulation of cardiac transcription factors could be a host mechanism necessary to stem the flow of cardiac specification, in order to halt any promiscuous cellular reprogramming and proliferation.

Interestingly, we saw a significant increase in GATA4 expression 23 days post-resection, indicating that GATA4 may be one of the major cardiac transcription factors involved with the specification of the cells responsible for the regeneration of the injured myocardium. This is in accordance with zebrafish heart regeneration, which requires the activation of specialized GATA4-expressing cardiomyocytes to replenish the resected myocardium (Kikuchi et al., 2010), and de novo mammalian cardiac specification, with GATA4 being one of several cardiac transcription factors needed for ectopic differentiation of mouse mesoderm or fibroblasts into cardiomyocytes (Ieda et al., 2010; Takeuchi and Bruneau, 2009).

In addition, we can also identify a proportion of cardiomyocytes in the injured newt ventricle that express Islet1. Islet1 has been shown to be a marker for cardiac progenitor cells and is an essential transcription factor in heart development (Brade et al., 2007; Cai et al., 2003; Moretti et al., 2006). However, the Islet1^{+ve} cell population in

the postnatal mammalian heart represents only a small fraction of cells and has never been observed in a functional cardiac regeneration model before (Genead et al., 2010; Laugwitz et al., 2005). It is interesting that we see dual expression of Islet1^{+ve} cardiomyocytes throughout the ventricle in adult newt hearts, whereas in mammalian species Islet1 expression within the heart is down-regulated soon after birth (Laugwitz et al., 2005). It has been suggested that Islet1 expression does remain in adult rat hearts but the expression is localized to cardiomyocyte labeled cells within the outflow tract (Genead et al., 2010).

Of further interest are the separate populations of proliferating GATA4 and Islet1 expressing cells in and around the area of regeneration that is not co-localized with cardiomyocyte markers. This indicates that there could be a population of cardiac progenitors with an earlier developmental phenotype up-regulated during the regeneration phase (Laugwitz et al., 2008; Zaglia et al., 2009). From where these cells derive still needs to be elucidated but we believe this is the first time that Islet1 positive cells can be linked to cardiac regeneration in vivo. As cardiomyocytes within the uninjured newt heart express Islet1, a scenario could exist where newt cardiomyocytes retain a higher level of plasticity, when compared to Islet1 negative cardiomyocytes found in mammals. This could make the Islet1 positive cardiomyocytes more open to dedifferentiation and proliferation, resulting in a greater contribution to the regeneration of the newt heart. This idea of a heterogeneous population has been suggested before in newt cardiomyocytes cultured in vitro and GATA4 expressing subepicardial ventricular cardiomyocytes in zebrafish cardiac regeneration (Bettencourt-Dias et al., 2003; Kikuchi et al., 2010).

The events leading to heart regeneration in newts are based on an increase in proliferation, coinciding with coordinated expression of cardiac transcription factors (Fig. 6). Discovering that the newt can replenish ventricular myocardium following resection will help compliment existing heart regeneration models already established in other organisms, like the teleost fish. In addition, urodele amphibians are evolutionary much closer to mammals than teleost fish, enhancing this organism's suitability as a comparative model to help optimize cardiac regeneration in mammals. Comparative and collaborative efforts using our newt heart regeneration model may go some way to resolving why damaged human hearts are unresponsive to potential regenerative signals following injury.

Supplementary materials related to this article can be found online at doi:10.1016/j.ydbio.2011.03.021.

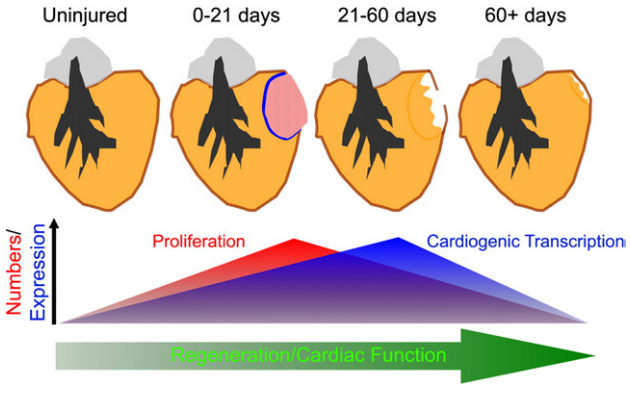

Fig. 6. Overview of newt cardiac regeneration of the ventricular myocardium. A diagrammatic representation depicting how the newt ventricle upon resection forms a fibrin clot that is underlined with fibrosis tissue. As time progresses the fibrin clot and fibrosis is replaced with invaginating cardiomyocytes, resulting in morphological and functional restoration of the heart. Coinciding with this is an increased rate of proliferative events and expression of cardiac transcription factors, which contributes to the mechanisms that lie behind the newly regenerated myocardium.

Author contributions

N.W. and J.I.M. designed the experiments. N.W., B.M. and J.I.M. devised and performed the surgical resection model. N.W., B.D., A.A. and J.I.M. performed the echocardiogram analysis. N.W. and J.I.M. performed the histology, immunofluorescence, all versions of PCR and data analysis. N.W., B.M., A.A. and J.I.M. wrote the paper.

Acknowledgments

We thank the Department of Molecular Biology and Functional Genomics at Stockholm University and the CMB at Karolinska Institute for their invaluable assistance. We are grateful to A. Eberle for technical assistance with qPCR, L. Wieslander for critically reading this paper, B. Borg for allowing us to house our newts in his aquaria facilities and J. Tibblin for her help with the Islet1 immunolabeling. We would also like to thank J. Nordholm, N. Schiller and H. Li for helping to design the degenerate primers to HAND2. This project was supported by grants from the Swedish Research Council and Swedish Heart–Lung Foundation to AA and Stockholm University, Åke Wiberg Stiftelse and Magn. Bergvalls Stiftelse to JIM.

References

Bader, D., Oberpriller, J.O., 1978. Repair and reorganization of minced cardiac muscle in the adult newt (*Notophthalmus viridescens*). J. Morphol. 155, 349–357.
Bartunek, J., Sherman, W., Vanderheyden, M., Fernandez-Aviles, F., Wijns, W., Terzic, A., 2009. Delivery of biologics in cardiovascular regenerative medicine. Clin. Pharmacol. Ther. 85, 548–552.
Becker, R.O., Chapin, S., Sherry, R., 1974. Regeneration of the ventricular myocardium in amphibians. Nature 248, 145–147.
Beltrami, A.P., Barlucchi, L., Torella, D., Baker, M., Limana, F., Chimenti, S., Kasahara, H., Rota, M., Musso, E., Urbanek, K., Leri, A., Kajstura, J., Nadal-Ginard, B., Anversa, P., 2003. Adult cardiac stem cells are multipotent and support myocardial regeneration. Cell 114, 763–776.
Beltrami, A.P., Urbanek, K., Kajstura, J., Yan, S.M., Finato, N., Bussani, R., Nadal-Ginard, B., Silvestri, F., Leri, A., Beltrami, C.A., Anversa, P., 2001. Evidence that human cardiac myocytes divide after myocardial infarction. N. Engl. J. Med. 344, 1750–1757.
Bergmann, O., Bhardwaj, R.D., Bernard, S., Zdunek, S., Barnabe-Heider, F., Walsh, S., Zupicich, J., Alkass, K., Buchholz, B.A., Druid, H., Jovinge, S., Frisen, J., 2009. Evidence for cardiomyocyte renewal in humans. Science 324, 98–102.
Bettencourt-Dias, M., Mittnacht, S., Brockes, J.P., 2003. Heterogeneous proliferative potential in regenerative adult newt cardiomyocytes. J. Cell Sci. 116, 4001–4009.
Boppart, S.A., Tearney, G.J., Bouma, B.E., Southern, J.F., Brezinski, M.E., Fujimoto, J.G., 1997. Noninvasive assessment of the developing *Xenopus* cardiovascular system using optical coherence tomography. Proc. Natl. Acad. Sci. USA 94, 4256–4261.
Brade, T., Gessert, S., Kuhl, M., Pandur, P., 2007. The amphibian second heart field: *Xenopus* islet-1 is required for cardiovascular development. Dev. Biol. 311, 297–310.
Brand, T., 2003. Heart development: molecular insights into cardiac specification and early morphogenesis. Dev. Biol. 258, 1–19.
Brockes, J.P., 1997. Amphibian limb regeneration: rebuilding a complex structure. Science 276, 81–87.
Brockes, J.P., Kumar, A., 2002. Plasticity and reprogramming of differentiated cells in amphibian regeneration. Nat. Rev. Mol. Cell Biol. 3, 566–574.
Cai, C.L., Liang, X., Shi, Y., Chu, P.H., Pfaff, S.L., Chen, J., Evans, S., 2003. Isl1 identifies a cardiac progenitor population that proliferates prior to differentiation and contributes a majority of cells to the heart. Dev. Cell 5, 877–889.
Chachques, J.C., 2009. Cellular cardiac regenerative therapy in which patients? Expert Rev. Cardiovasc. Ther. 7, 911–919.
Chen, J.N., Fishman, M.C., 1996. Zebrafish tinman homolog demarcates the heart field and initiates myocardial differentiation. Development 122, 3809–3816.
Cleaver, O.B., Patterson, K.D., Krieg, P.A., 1996. Overexpression of the tinman-related genes XNkx-2.5 and XNkx-2.3 in *Xenopus* embryos results in myocardial hyperplasia. Development 122, 3549–3556.
Flink, I.L., 2002. Cell cycle reentry of ventricular and atrial cardiomyocytes and cells within the epicardium following amputation of the ventricular apex in the axolotl, *Amblystoma mexicanum*: confocal microscopic immunofluorescent image analysis of bromodeoxyuridine-labeled nuclei. Anat. Embryol. Berl. 205, 235–244.
Genead, R., Danielsson, C., Andersson, A.B., Corbascio, M., Franco-Cereceda, A., Sylven, C., Grinnemo, K.H., 2010. Islet-1 cells are cardiac progenitors present during the entire lifespan: from the embryonic stage to adulthood. Stem Cells Dev. 19, 1601–1615.
Genovese, J., Cortes-Morichetti, M., Chachques, E., Frati, G., Patel, A., Chachques, J.C., 2007. Cell based approaches for myocardial regeneration and artificial myocardium. Curr. Stem Cell Res. Ther. 2, 121–127.
Harvey, R.P., 2002. Molecular determinants of cardiac development and congenital disease. In: Rossant, J., Tam, P.L. (Eds.), Mouse Development: Patterning, Morphogenesis and Organogenesis. Academic Press, San Diego, California, pp. 331–370.

Ieda, M., Fu, J.D., Delgado-Olguin, P., Vedantham, V., Hayashi, Y., Bruneau, B.G., Srivastava, D., 2010. Direct reprogramming of fibroblasts into functional cardiomyocytes by defined factors. Cell 142, 375–386.

Iten, L.E., Bryant, S.V., 1973. Forelimb regeneration from different levels of amputation in the newt, *Notophthalmus viridescens*: length, rate, and stages. Dev. Genes Evol. 173, 263–282.

Jobsis, P.D., Ashikaga, H., Wen, H., Rothstein, E.C., Horvath, K.A., McVeigh, E.R., Balaban, R.S., 2007. The visceral pericardium: macromolecular structure and contribution to passive mechanical properties of the left ventricle. Am. J. Physiol. Heart Circ. Physiol. 293, H3379–H3387.

Jopling, C., Sleep, E., Raya, M., Marti, M., Raya, A., Belmonte, J.C., 2010. Zebrafish heart regeneration occurs by cardiomyocyte dedifferentiation and proliferation. Nature 464, 606–609.

Kasahara, H., Ueyama, T., Wakimoto, H., Liu, M.K., Maguire, C.T., Converso, K.L., Kang, P.M., Manning, W.J., Lawitts, J., Paul, D.L., Berul, C.I., Izumo, S., 2003. Nkx2.5 homeoprotein regulates expression of gap junction protein connexin 43 and sarcomere organization in postnatal cardiomyocytes. J. Mol. Cell. Cardiol. 35, 243–256.

Kikuchi, K., Holdway, J.E., Werdich, A.A., Anderson, R.M., Fang, Y., Egnaczyk, G.F., Evans, T., Macrae, C.A., Stainier, D.Y., Poss, K.D., 2010. Primary contribution to zebrafish heart regeneration by gata4(+) cardiomyocytes. Nature 464, 601–605.

Laube, F., Heister, M., Scholz, C., Borchardt, T., Braun, T., 2006. Re-programming of newt cardiomyocytes is induced by tissue regeneration. J. Cell Sci. 119, 4719–4729.

Laugwitz, K.L., Moretti, A., Caron, L., Nakano, A., Chien, K.R., 2008. Islet1 cardiovascular progenitors: a single source for heart lineages? Development 135, 193–205.

Laugwitz, K.L., Moretti, A., Lam, J., Gruber, P., Chen, Y., Woodard, S., Lin, L.Z., Cai, C.L., Lu, M.M., Reth, M., Platoshyn, O., Yuan, J.X., Evans, S., Chien, K.R., 2005. Postnatal isl1+ cardioblasts enter fully differentiated cardiomyocyte lineages. Nature 433, 647–653.

Martin, C.M., Meeson, A.P., Robertson, S.M., Hawke, T.J., Richardson, J.A., Bates, S., Goetsch, S.C., Gallardo, T.D., Garry, D.J., 2004. Persistent expression of the ATP-binding cassette transporter, Abcg2, identifies cardiac SP cells in the developing and adult heart. Dev. Biol. 265, 262–275.

Moretti, A., Caron, L., Nakano, A., Lam, J.T., Bernshausen, A., Chen, Y., Qyang, Y., Bu, L., Sasaki, M., Martin-Puig, S., Sun, Y., Evans, S.M., Laugwitz, K.L., Chien, K.R., 2006. Multipotent embryonic isl1+ progenitor cells lead to cardiac, smooth muscle, and endothelial cell diversification. Cell 127, 1151–1165.

Morrison, J.I., Borg, P., Simon, A., 2010. Plasticity and recovery of skeletal muscle satellite cells during limb regeneration. FASEB J. 24, 750–756.

Morrison, J.I., Loof, S., He, P., Simon, A., 2006. Salamander limb regeneration involves the activation of a multipotent skeletal muscle satellite cell population. J. Cell Biol. 172, 433–440.

Mummery, C.L., Davis, R.P., Krieger, J.E., 2010. Challenges in using stem cells for cardiac repair. Sci. Transl. Med. 2 27ps17.

Neff, A.W., Dent, A.E., Armstrong, J.B., 1996. Heart development and regeneration in urodeles. Int. J. Dev. Biol. 40, 719–725.

Oberpriller, J.O., Oberpriller, J.C., 1974. Response of the adult newt ventricle to injury. J. Exp. Zool. 187, 249–253.

Oberpriller, J.O., Oberpriller, J.C., Matz, D.G., Soonpaa, M.H., 1995. Stimulation of proliferative events in the adult amphibian cardiac myocyte. Ann. N.Y. Acad. Sci. 752, 30–46.

Oh, H., Bradfute, S.B., Gallardo, T.D., Nakamura, T., Gaussin, V., Mishina, Y., Pocius, J., Michael, L.H., Behringer, R.R., Garry, D.J., Entman, M.L., Schneider, M.D., 2003. Cardiac progenitor cells from adult myocardium: homing, differentiation, and fusion after infarction. Proc. Natl. Acad. Sci. USA 100, 12313–12318.

Pasumarthi, K.B., Field, L.J., 2002. Cardiomyocyte cell cycle regulation. Circ. Res. 90, 1044–1054.

Porrello, E.R., Mahmoud, A.I., Simpson, E., Hill, J.A., Richardson, J.A., Olson, E.N., Sadek, H.A., 2011. Transient regenerative potential of the neonatal mouse heart. Science 331, 1078–1080.

Poss, K.D., Wilson, L.G., Keating, M.T., 2002. Heart regeneration in zebrafish. Science 298, 2188–2190.

Reffelmann, T., Konemann, S., Kloner, R.A., 2009. Promise of blood- and bone marrow-derived stem cell transplantation for functional cardiac repair: putting it in perspective with existing therapy. J. Am. Coll. Cardiol. 53, 305–308.

Saadane, N., Alpert, L., Chalifour, L.E., 1999. Expression of immediate early genes, GATA-4, and Nkx-2.5 in adrenergic-induced cardiac hypertrophy and during regression in adult mice. Br. J. Pharmacol. 127, 1165–1176.

Srivastava, D., Cserjesi, P., Olson, E.N., 1995. A subclass of bHLH proteins required for cardiac morphogenesis. Science 270, 1995–1999.

Takeuchi, J.K., Bruneau, B.G., 2009. Directed transdifferentiation of mouse mesoderm to heart tissue by defined factors. Nature 459, 708–711.

Torella, D., Ellison, G.M., Karakikes, I., Nadal-Ginard, B., 2007. Growth-factor-mediated cardiac stem cell activation in myocardial regeneration. Nat. Clin. Pract. Cardiovasc. Med. 4 (Suppl 1), S46–S51.

van Laake, L.W., Passier, R., Monshouwer-Kloots, J., Verkleij, A.J., Lips, D.J., Freund, C., den Ouden, K., Ward-van Oostwaard, D., Korving, J., Tertoolen, L.G., van Echteld, C.J., Doevendans, P.A., Mummery, C.L., 2007. Human embryonic stem cell-derived cardiomyocytes survive and mature in the mouse heart and transiently improve function after myocardial infarction. Stem Cell Res. 1, 9–24.

Vascotto, S.G., Beug, S., Liversage, R.A., Tsilfidis, C., 2005. Nvbeta-actin and NvGAPDH as normalization factors for gene expression analysis in limb regenerates and cultured blastema cells of the adult newt, *Notophthalmus viridescens*. Int. J. Dev. Biol. 49, 833–842.

Weber, K.T., 1989. Cardiac interstitium in health and disease: the fibrillar collagen network. J. Am. Coll. Cardiol. 13, 1637–1652.

Yuasa, S., Fukuda, K., Tomita, Y., Fujita, J., Ieda, M., Tahara, S., Itabashi, Y., Yagi, T., Kawaguchi, H., Hisaka, Y., Ogawa, S., 2004. Cardiomyocytes undergo cells division following myocardial infarction is a spatially and temporally restricted event in rats. Mol. Cell. Biochem. 259, 177–181.

Zaglia, T., Dedja, A., Candiotto, C., Cozzi, E., Schiaffino, S., Ausoni, S., 2009. Cardiac interstitial cells express GATA4 and control dedifferentiation and cell cycle re-entry of adult cardiomyocytes. J. Mol. Cell. Cardiol. 46, 653–662.